Comparisons of Shear Characteristics of Laboratory and Field-Compacted Soil

S. O. NWABOUKEI and C. W. LOVELL

ABSTRACT

Shear strength parameters of soils in compacted embankments are usually estimated from tests on laboratory-compacted soils and infrequently on field-compacted soils. However, owing to the difference in the compactive modes that may be used and the variability in the soil that may be employed, it is necessary to define the effect of the various compaction variables on the shear strength characteristics of compacted soils. A series of unconsolidated-undrained tests on as-compacted specimens and consolidated-undrained tests on back-pressured-to-saturation specimens with pore pressure measurements was performed on laboratory- and field-compacted St. Croix (Indiana) clay in a triaxial cell. The results show similarity in their shear strength behavior. Procedures are suggested for adjusting laboratory results to enable an engineer to predict effectively the shear strength behavior of field-compacted soils for both short- and long-term conditions.

Compaction has long been recognized as the most economical mechanical procedure for improving the shear strength, compressibility, and permeability characteristics of a soil. Usually, adequate performance of compacted embankments is effected by placing limits on suitable placement compaction variables, such as moisture content, dry density, compaction effort, and type of compaction equipment. However, with the increasing demand for the construction of higher embankments, the need arises to specify placement conditions that will control the shear strength, compressibility, and volume changes such that safe and economical embankments can be constructed for both the short- and long-term periods.

In this study the effects of compaction variables on the short- and long-term shear strength behavior of laboratory- and field-compacted plastic residual clayey soils were investigated. The short-term strength behavior was simulated by unconsolidated undrained tests on laboratory- and field-compacted soils subjected to various confining stresses. The long-term shear strength behavior was also simulated by isotropically consolidated undrained tests with pore pressure measurements. Using statistical techniques, prediction models for various shear strength parameters as functions of the relative basic compaction variables were developed.

Procedures are also outlined so that an engineer can conveniently adjust laboratory measurements with a view to predicting field shear strength behavior of similar soils.

EXPERIMENTAL PROCEDURE

Major Factors

Soil Description

The soil used for this study (field- and laboratory-compacted) was St. Croix clay, a residual soil of sandstone and shale origin taken from a cut area about 6.5 km south of St. Croix, Indiana. The results of the classification tests conducted on the test pads and laboratory test soils are given in Table 1.

TABLE 1 Properties and Classifications of St. Croix Clay

Category	Classification or Value: Laboratory Soil	Classification or Value: Test Pad Soil
Liquid limit	52	40 (30-53.2)
Plastic limit	23	18.4 (16.7-21.3)
Plastic index	29	21.9 (16.4-29)
Shrinkage limit	12	11.8
Specific gravity	2.8	2.79
Clay fraction (<2 μm)%	40	34
Skempton's activity	0.73	0.65
Unified soil classification	CH	CL
AASHTO soil classification	A-7-6	A-6

Laboratory Compaction

The laboratory triaxial samples were prepared using the California Kneading Compactor. This compactor was chosen in order to approximate field rolling more appropriately, in terms of the shearing strains and load patterns that were to be exerted in the field. Work applied to the soil was deduced from the load and displacement measurements of the kneading compactor foot. The kneading foot pressures were chosen to fit the dry density versus moisture content relationships obtained for the modified Proctor compaction (AASHTO 7-180-70), standard Proctor compaction, and a low energy level corresponding to 15 blows for each of the three layers used.

The following codes were adopted for identifying the laboratory-compacted soil, tested under unconsolidated undrained conditions. C0, C1, C2, and C3 refer to confining pressures of 0 kPa, 138 kPa, 276 kPa, and 414 kPa, respectively. L, S, and M represent low, standard, and modified compaction energies. The numbers after the preceding letters refer to the degree of saturation, whereas the last number is used for differentiating samples with identical initial conditions (e.g., C0-L1-2). Also, for samples tested under isotropically consolidated undrained conditions, L, S, and M are as indicated previously. D, O, and W refer to moisture content conditions of dry of optimum, optimum, and wet of optimum, respectively. The numbers 1, 2, and 3 are used for differentiating samples with identical initial conditions. The number in brackets indicates the effective consolidation pressure (in kPa) for that sample [e.g., LO1(69)]. Details of test procedures are outlined in Weitzel and Lovell (1) and Johnson and Lovell (2).

Field Compaction

Ten test pads were used in the field studies. Five test pads at various moisture contents were com-

pacted by a Raygo Rascal Model 420C vibratory drum compactor, whereas the other five test pads at similar moisture contents were rolled with a Caterpillar Model 825 tamping foot roller.

The test pads were divided into a 0.6 m x 0.6 m grid framework with samples obtained after 4, 8, and 16 passes. Sampling was accomplished by driving thin-walled stainless steel tubes into the grid-patterned test sections. Field densities and moisture contents for the various test pads at the desired number of passes were determined by nuclear density equipment and the Speedy Moisture Meter.

For the field-compacted soils, the following coding was used for sample identification. R and C represent the Rascal Roller and Caterpillar Tamping Roller. The number immediately thereafter refers to the water content level. A, B, and C represent the compaction energy levels of 4, 8, and 16 passes, respectively. The subsequent number was used to differentiate samples with identical initial conditions, while the last number in brackets refers to the confining pressure or isotropic consolidation pressure for the unconsolidated undrained or consolidated undrained tests, respectively. Details of test procedures are outlined in Liang and Lovell (3).

TEST RESULTS AND ANALYSIS

Dry Density and Moisture Content Relationships

Figure 1 shows the dry density and moisture content relationships for the Raygo Rascal vibratory drum-compacted St. Croix clay at 4, 8, and 16 passes with respect to impact-compacted test pad St. Croix clay. The 4 passes curve corresponds approximately to the low energy impact curve; the 8 passes curve lies between the low energy and the Standard Proctor, whereas the 16 passes curve lies above the Standard Proctor curve.

Figure 2 shows a similar relationship for the Caterpillar tamping roller- and impact-compacted test pad St. Croix clay. The 4 passes curve lies above the low energy curve whereas the 8 and 16 passes curves are between the standard and modified Proctor curves.

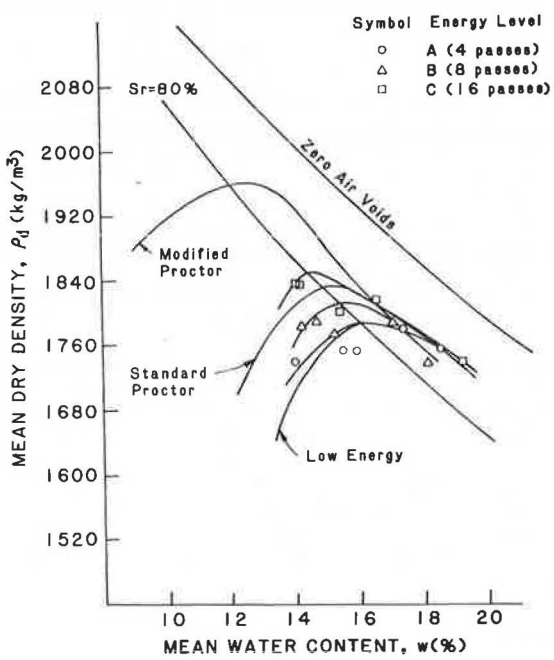

FIGURE 1 Correspondence between Rascal Roller and Impact Method.

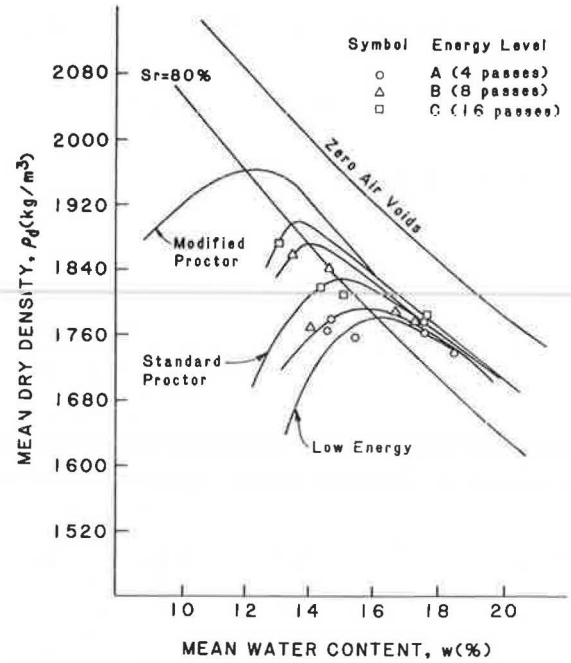

FIGURE 2 Correspondence between Caterpillar Roller and impact method.

Figure 3 also shows the dry density versus moisture content relationship for the kneading and impact compacted laboratory St. Croix clay. In order to fit the kneading compaction results to a constant nominal energy Proctor curve, less energy was re-

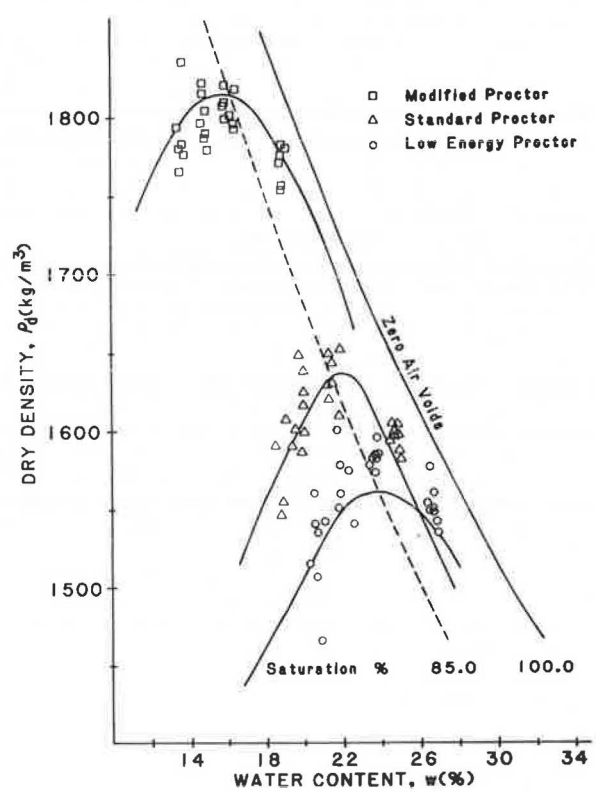

FIGURE 3 Dry density-water content relationship for triaxial test samples before testing.

quired as water content increased, indicating the generally higher efficiency of the kneading mode over the impact method for the soils investigated.

Using a statistical regression technique, dry density prediction models were developed for the laboratory-and field-compacted soils. Dry densities (ρ_d) at wet of optimum moisture contents were found to be independent of the compactive effort, whereas dry of optimum moisture content dry densities were functions of the compactive pressure (P_c) and moisture content (w).

The prediction models, where ρ_d is in units of kg/m³, w in percent, and P_c in kPa, are as follows:

1. Wet of optimum moisture content:
   (a) Laboratory-compacted soil

$$\rho_d = 961.8 + 15{,}564.6/w \quad (1)$$

   (b) Field-compacted soil

$$\rho_d = 1{,}273.05 + 8{,}797.21/w \quad (2)$$

The coefficients of determination (R^2) for 1(a) and 1(b) are 0.99 and 0.88, respectively.

2. Dry of optimum moisture content:
   (a) Laboratory-compacted soil

$$\rho_d = 1{,}566.8 + 62.42\sqrt{P_c}/w + 0.00214\sqrt{P_c w^2} + 0.0031wP_c - 2{,}617.4/w \quad (3)$$

   (b) Field-compacted soil

$$\rho_d = 1{,}929.69 + 211.6\sqrt{P_c}/w + 0.0016\sqrt{P_c w^2} - 0.0096wP_c - 6{,}816.83/w \quad (4)$$

The coefficients of determination (R^2) for 2(a) and 2(b) are 0.93 and 0.74, respectively.

The above models are valid only over the moisture range for which they were determined.

Compactive Prestress

Compactive prestress that is analogous to preconsolidation pressure in geologic deposits reflects the portion of the compactive pressure effectively transmitted to the soil skeleton. The shear strength and compressibility response of a compacted soil mass is highly dependent on this parameter. Results from the studies carried out by Lin and Lovell (4) and DiBernardo and Lovell (5), using the relevant compaction variables as independent variables, yield the following relationships for the compactive prestresses (P_s) for the laboratory- and field-compacted soils.

(a) Laboratory-compacted soil

$$P_s = -343.52 - 0.002w^2P_c + 48.91P_c^{1/2} \quad (5)$$

(b) Field-compacted soil

$$P_s = -160.99 - 0.00063w^2P_c + 27.04P_c^{1/2} \quad (6)$$

where the units of P_s and P_c are in kPa, and w is in percent.

The coefficients of determination for a and b are 0.88 and 0.87, respectively. A detailed treatment of compactive prestress is given by Lovell (6).

Unconsolidated Undrained Test

Stress-Strain Behavior

A compacted soil is primarily a three-phase system that consists of soil grains or aggregates, water, and air in which densification of the soil is achieved by a reduction of air voids at constant water content. Hodek and Lovell (7) developed a mechanism of clay soil densification that accounted for the precompaction soil preparation and conditioning as well as the soil interactions during compaction. Compacted clay soil was considered to be formed of soil aggregations of clay particles, which at dry of optimum moisture content were shrunken, hard, and brittle. The compaction forces move these aggregates around and may even break them, resulting in a system with maximum volume of large pores and minimum volume of small pores. In contrast, on the wet of optimum moisture content the clay aggregates are swollen and plastic, with the compaction forces being able to move the aggregates closer together and deform them to yield a system with few large pores and many small ones.

The stress-strain and volumetric strain behavior are therefore dependent on the soil type, compaction variables (compaction effort, compaction moisture content, and compaction mode), confining pressure, and the fabric generated in the soil.

Typical stress-strain and volumetric strain behavior of the field- and laboratory (kneading)-compacted soils are shown in Figures 4 and 5, respectively, and properties of those soil samples tested are given in Table 2. The results indicate that dry of optimum samples, with large interaggregate voids and negative pore pressures, exhibit a more brittle behavior at low confining pressure. Consequently, low strains are required for the mobilization of the total shearing resistance. Also, the stress-strain

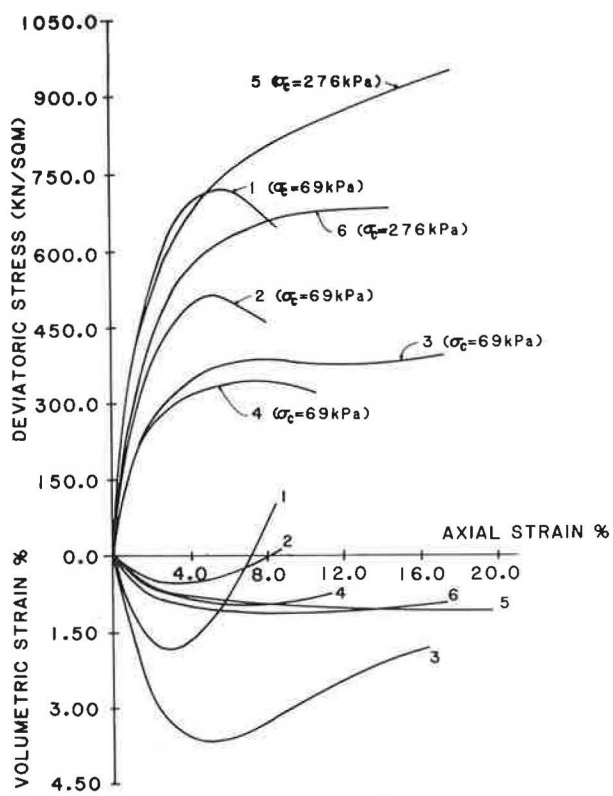

FIGURE 4 Axial stress and volumetric strain versus axial strain for field-compacted samples.

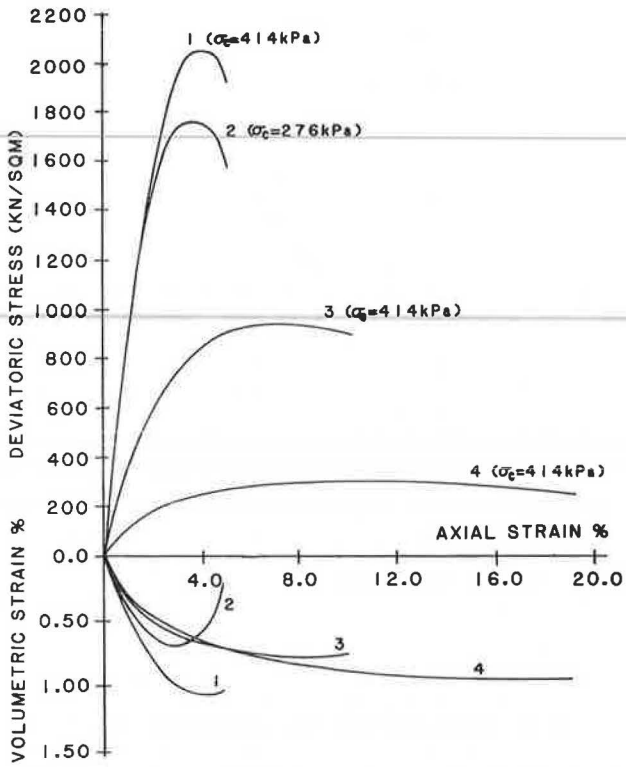

FIGURE 5 Axial strain and volumetric strain versus axial strain for laboratory-compacted samples.

TABLE 2 Properties of the Soil Samples Whose Test Results are Shown in Figures 4, 5, 12, and 13

Figure No.	Curve No.	Sample No.	Dry Density (kg/m^3)	Water Content (%)
4	1	R2B7(69)	1842.9	14.10
	2	C2B3(69)	1824.2	14.85
	3	R3B10(69)	1724.8	15.40
	4	C3B3(69)	1744.9	18.16
	5	R2C4(276	1831.0	15.44
	6	C2C6(276)	1843.7	15.00
5	1	C3-M2-2	1819.8	15.00
	2	C2-M2-1	1815.5	15.05
	3	C3-M4-1	1781.4	18.95
	4	C3-S4-1	1587.7	25.09
12	1	SO2(138)	1651-9	22.39
	2	SD2(138)	1600.8	19.37
	3	SW2(138)	1579.0	24.92
13	1	C3B6(138)	1794.07	13.64
	2	R3C9(138)	1804.50	16.37
	3	C3C1(138)	1830.96	15.01
	4	R3B7(138)	1749.80	13.57

behavior of the dry of optimum samples are dependent on the ensuing volumetric changes, with the maximum amount of densification being attained quickly and subsequently accompanied by dilation. Peak deviator stresses are then reached shortly thereafter. At a low compaction energy level, high confining pressures induce plastic behavior in St. Croix clay, regardless of the moisture content.

The results also indicate that the volume change due to shear is related to the compactive prestress (P_S) induced in the sample, with volumetric strain at failure decreasing with increasing "overconsolidation ratio" (P_S/σ_C), where σ_C is confining pressure. As water content increases from dry of optimum, the low energy and Standard Proctor energy samples exhibit a more plastic behavior, due in part to the reduced prestress. The volumetric strain at failure also decreases with increased degree of saturation. Samples wet of optimum moisture content, subjected to high confining pressures, may experience enough compression to enable the soil specimens to approach saturation and thereby yield low volumetric strains at failure.

At dry of optimum moisture content, the modified Proctor energy samples have their soil aggregations packed into a dense configuration, have high prestress values, and consequently exhibit a stiff and brittle stress-strain behavior with dilatant tendencies. At wet of optimum moisture content, the samples have lower prestress values and exhibit plastic stress-strain behaviors and low volumetric strain behaviors at failure. The volumetric strain behavior as functions of compaction water content and confining pressure is shown in Figure 6 for laboratory-compacted samples.

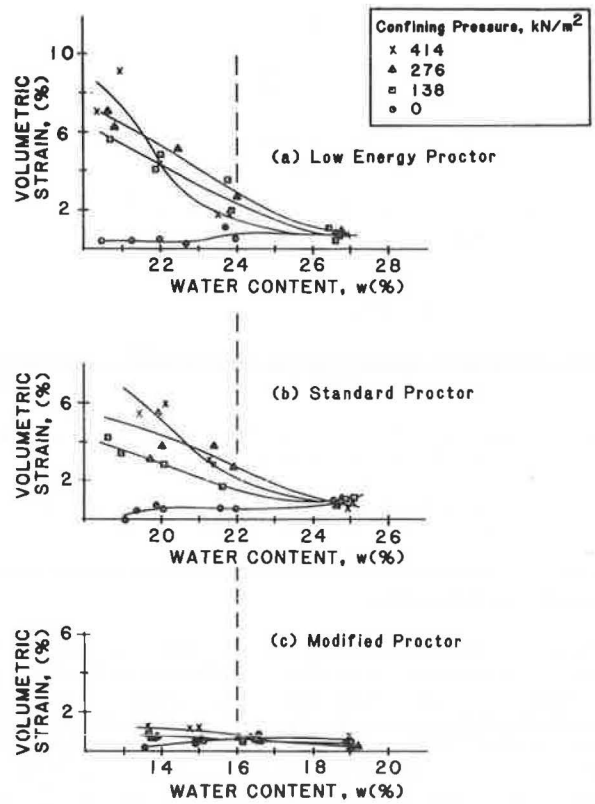

FIGURE 6 Water content versus volumetric strain at failure for laboratory-compacted samples.

The volumetric strain due to shear as functions of compaction water content and confining pressure for the Caterpillar tamping roller is shown in Figure 7. A general trend, in which the volumetric strains at failure decrease with water content, can be observed. Similar results were obtained for the Raygo Rascal Rollers. Consequently, during shear, dry of optimum samples with higher prestress, higher negative pore pressure, and large interaggregate voids exhibit higher deviator stresses and volumetric strains at failure. Low axial strains are required for the mobilization of the total shearing resistance. Wet of optimum moisture content samples (characterized by lower prestress values), many small pores filled with incompressible water, and

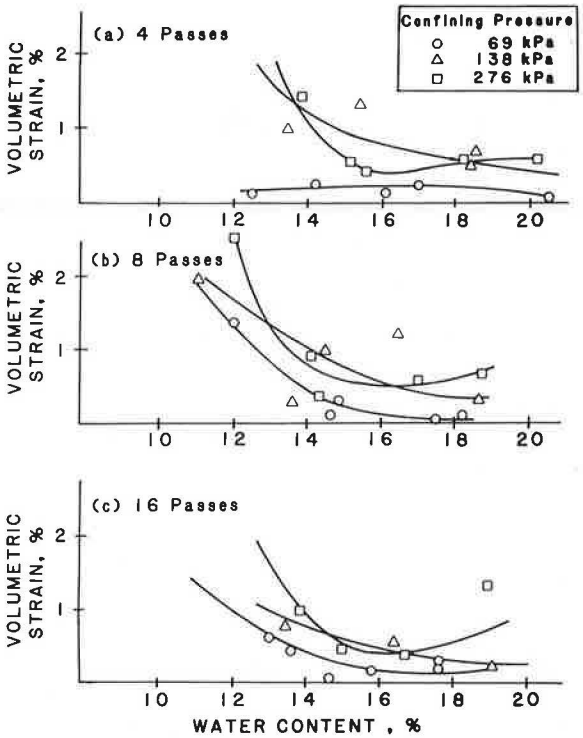

FIGURE 7 Water content versus volumetric strain during application of confining pressure for Caterpillar samples.

occluded air exhibit lower total shearing resistances and volumetric strains at failure. High axial strains are required for the mobilization of these parameters.

Unconsolidated-Undrained Strength

Dacruz (8) obtained a linear relationship between the product of void ratio at failure (e_f) and square root of degree of saturation at failure (S_f) and the logarithm of one-half the principal stress difference (q_c) at failure. Similar results were obtained in this study for the field-compacted soil.

$$q_c = 4.256 - 3.88e_f \sqrt{S_f} \quad (7)$$

where the units of q_c are in kPa. A coefficient of determination of 0.66 was obtained, which is low but acceptable.

The as-compacted undrained strength (q_c) models, as functions of the relevant initial compaction variables, where the unit of q_c is in kPa, ρ_d is in kg/m^3, w and S are in percent, are given:

(a) Laboratory-compacted soil

$$q_c = -1{,}878.2 + 51.54w - 0.06\rho_d w + 1.39w^2 + 76.91(1 - S_i/100)\sqrt{\sigma_c} + 3.68\rho_d \sqrt{S_i}/w \quad (8)$$

(b) Field-compacted soil

$$q_c = -6{,}980 + 636.21w + 8.3w^2 - 0.155\rho_d w + 112/1\ (1 - S_i/100)\sqrt{\sigma_c} + 3.6\rho_d \sqrt{S_i}/w \quad (9)$$

The coefficients of determination of the undrained strengths of the laboratory- and field-compacted soils are 0.983 and 0.72, respectively.

These prediction models can be expressed in terms of initial void ratio (e_o), moisture content, and confining pressures, because

$$\rho_d = G_s\rho_w/1 + e_o \quad (10)$$

and

$$S_i = wG_s/e_o \quad (11)$$

where G_s is the specific quantity of solids and ρ_w is the density of water.

Figures 8 and 9 show typical relationships using the prediction models for both the laboratory and field-compacted soils for a given void ratio. The differences in the strengths that can be predicted from both models stem from the following factors: (a) differences in the type of soil (see Table 1), (b) differences in the compactive prestress induced by the various compaction methods, and (c) differences in the soil fabric created.

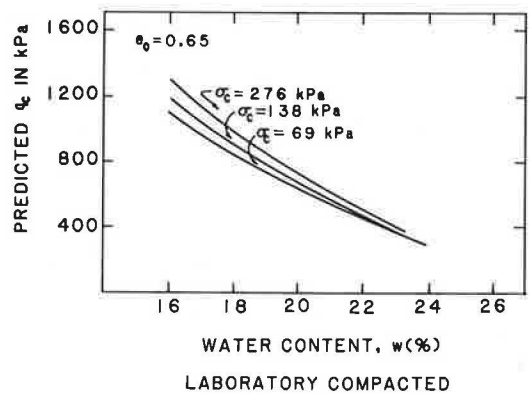

FIGURE 8 Predicted laboratory as-compacted strength-water content relationship at a constant initial void ratio.

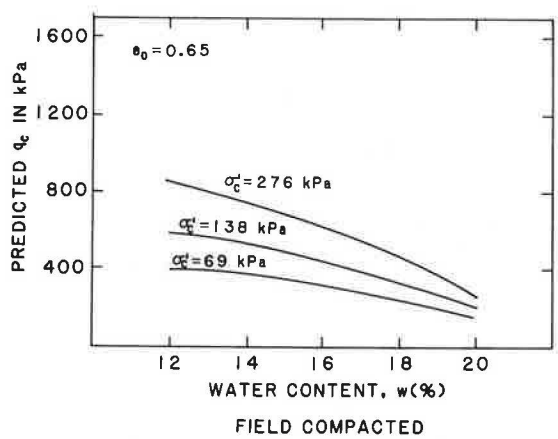

FIGURE 9 Predicted field as-compacted strength-water content relationship at a constant initial void ratio.

From Figures 8 and 9 it can be observed that at a given void ratio and under specific confining pressure, the undrained strength decreases with increasing water content. The undrained strength increases with confining pressure at dry of optimum while it attains an approximately constant value at wet of optimum (high degree of initial saturation) irrespective of the confining pressures.

CONSOLIDATED UNDRAINED TESTS

Volume Change Behavior Under Saturation and Consolidation

To satisfy design criteria for the long-term performance of a compacted embankment with respect to deformation and strength, there is the need to control the volume changes that are likely to occur due to loading and saturation. This has been approximated by back pressure saturation of the compacted samples and isotropic consolidation to equivalent embankment pressures of 69 kPa, 138 kPa, and 276 kPa.

A similarity does exist in the volume change behaviors of the specimens prepared by the three modes of laboratory and field compaction for a given consolidation pressure, that is, the volumetric strain decreases (more swell) with decreasing initial void ratio. Samples of soils compacted under high energy levels (16 passes for the Rascal and Caterpillar Compactors and Kneading compaction corresponding to the Modified Proctor) swelled more under low confining pressure. Samples compacted at low energy levels showed increased compression tendencies with increased confining pressures.

The test results also indicate that for a given void ratio, volume changes decreased (more swell) in the following order: laboratory kneading, Caterpillar- and Rascal-compacted samples. This is a manifestation of the induced prestress and the resultant fabric of the compacted soils.

A statistical technique using the basic independent variables of water content (w), dry density (initial void ratio, e_o), effective confinement (σ_c'), and compactive prestress (P_s) were used in deriving regression models for the volumetric strains due to saturation and consolidation for both the laboratory- and field-compacted soils. These prediction models, where the units of σ_c' and P_s are in kPa and w is in percent, are as follows:

(a) Laboratory-compacted soils

$$(\Delta V/V_o)\% = -9.4 + 2.9e_o\sqrt{\sigma_c'} - 0.40P_s - 0.00276w\sigma_c' \quad (12)$$

(b) Field-compacted soils

$$(\Delta V/V_o)\% = -0.166 + 2.47e_o\sqrt{\sigma_c'} - 0.365P_s - 0.00263w\sigma_c' \quad (13)$$

The coefficients of determination (R^2) for the laboratory- and field-compacted soil volumetric strain prediction models are 0.95 and 0.72, respectively. The constant terms in these prediction models give indications of the free swell capacities of the soils.

The regression models are shown graphically in Figures 10 and 11 for the ascribed void ratio. Observe that St. Croix clay exhibits more swelling tendency as compactive prestress increases. Also volume changes increase (more compression) with increasing confining pressure and increasing initial water content. The highest swell occurs at the lowest confining pressure and highest compactive prestress for a given water content and dry density.

Stress-Strain and Pore Pressure Responses

Typical stress-strain and pore pressure-strain relationships for the laboratory- and field-compacted soils (back-pressured to saturation and tested under consolidated undrained conditions) are given in Figures 12 and 13. The stress-strain behavior and pore

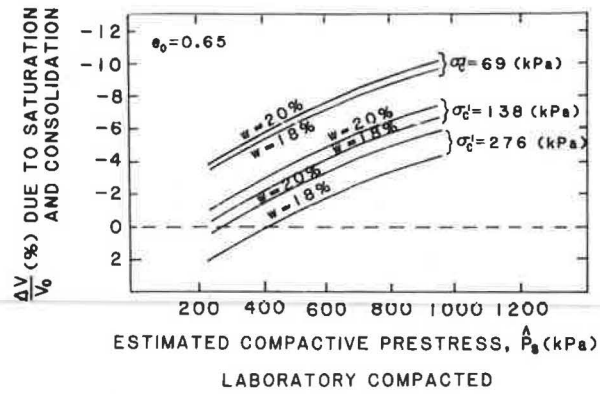

FIGURE 10 Prediction of laboratory percent volume change due to saturation and consolidation at a constant initial void ratio.

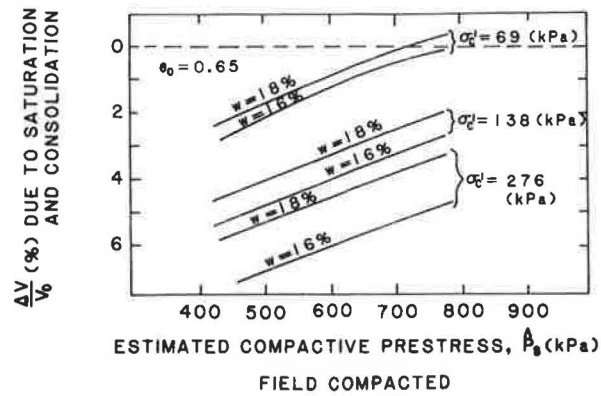

FIGURE 11 Prediction of field volume change due to saturation and consolidation at a constant initial void ratio.

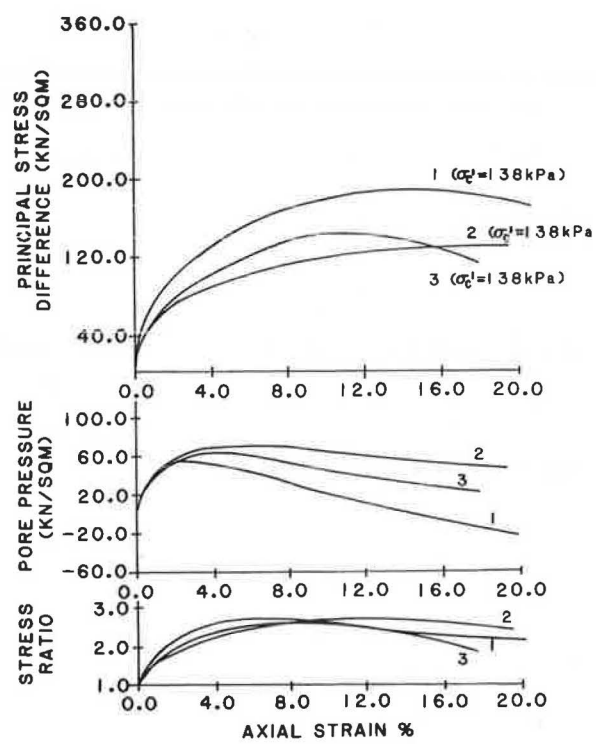

FIGURE 12 Results from $\overline{CIU}$ triaxial tests for laboratory-compacted samples.

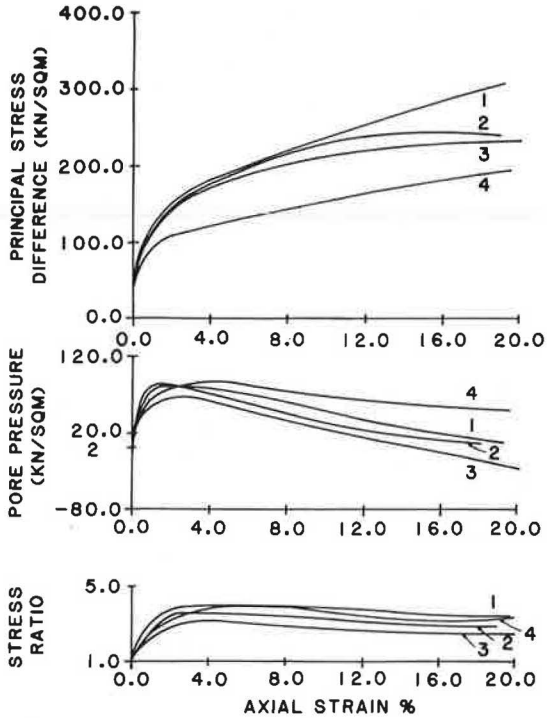

FIGURE 13 Results from $\overline{CIU}$ triaxial tests for field-compacted samples.

pressure responses are dependent on the compaction moisture content, void ratio (dry density), confining pressure, compactive prestress, and the fabric created.

A statistical regression analysis was applied to define the independent variables that control Skempton's A parameter at failure (A_f) for the laboratory- and field-compacted soils. The regression models, in which the units of ρ_d are in kg/m³ and S_i in percent, are as follows:

(a) Laboratory-compacted soil

$$A_f = 2.34 + 0.56/e_o - 0.0189 \times 10^{-4}\rho_d \sqrt{S_i} - 0.246 \log OCR \quad (14)$$

(b) Field-compacted soil

$$A_f = 2.05 + 0.73/e_o - 0.232 \times 10^{-4}\rho_d \sqrt{S_i} - 0.382 \log OCR \quad (15)$$

R^2 values for the A_f parameter for the laboratory- and field-compacted soils are 0.72 and 0.63, respectively. Typical results for a given initial degree of saturation are given in Figures 14 and 15. Skempton's A parameter at failure decreases with an increase in overconsolidation ratio. This is in agreement with the results presented by Henkel (9) for saturated remolded clays. The results also indicate an increase in A_f values with increase in void ratio (decrease in dry density) for a given degree of saturation and OCR. Thus considering two samples compacted to the same dry density, but different initial degrees of saturation, the one with the lower degree of initial saturation will swell more on saturation under a given confining pressure, and compress more under shear, and consequently produce a higher A_f value.

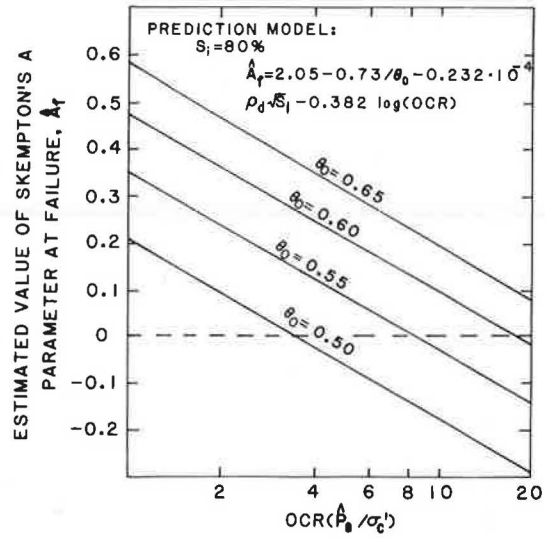

FIGURE 14 Field Skempton's A parameter at failure versus OCR at a constant initial saturation.

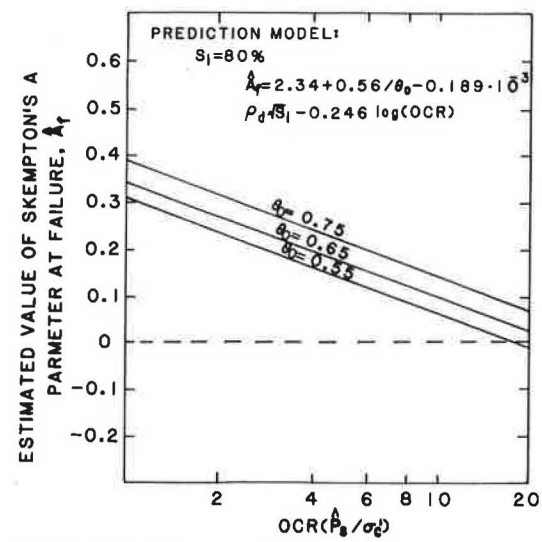

FIGURE 15 Laboratory Skempton's A parameter at failure versus OCR at a constant initial saturation.

EFFECTIVE STRESS STRENGTH PARAMETERS

The effective stress strength parameters of the laboratory- and field-compacted soils were obtained from the modified Coulomb plots in which the values of $q_f = (\sigma_1 - \sigma_3)f/2$ and $p_f' = (\sigma_1' + \sigma_3')f/2$ had been subjected to a regression analysis. This procedure was found to be useful, especially for the field-compacted soil where the initial compaction conditions were so varied.

The results indicate that the effective strength parameters depend on the following pertinent variables:

1. Initial void ratio,
2. Compactive prestress,
3. Consolidation pressure (equivalent embankment pressure), and
4. The soil fabric created by the various compaction modes and the modification thereof from the effects of embankment pressure and environmental

changes that were simulated in the laboratory by saturation and consolidation.

For the laboratory-compacted soil, the variations in the effective stress friction angles were small for the compaction and consolidation conditions investigated. The measured effective stress friction angle varied from 18.9 to 21.4 degrees. These friction angles are the result of a complex interaction between compressibility, shear strength, and pore water pressure. A value of $\phi' = 20 \pm 1.3$ degrees is suggested for the compaction and consolidation conditions covered in this study.

However, for the field-compacted soil, a regression model for the effective stress friction angle (ϕ') was developed as follows:

$$\phi' = 47.56 - 2.112w - 2.625w \log e_o \quad (16)$$

where w is the compaction water content (percent). The coefficient of multiple determination for this relationship is 0.89. The effective stress friction angle decreases with increase in compaction moisture content, which is attributable to the more parallel fabric created, lower prestress values, and consequently higher pore pressures. Higher ϕ' values were obtained for the dry of optimum moisture content samples due to their less parallel fabric, higher particle interference during shear, and higher dilatancy tendencies resulting from their higher prestress values.

Using the initial moisture content (w, percent) and void ratio (e_o), regression models were developed for the effective stress-strength intercept (c', kPa) for the laboratory- and field-compacted soils.

(a) Laboratory-compacted soil

$$c' = 1.71 - 3.83w \log e_o \quad (17)$$

(b) Field-compacted soil

$$c' = -102.79 + 11.208w + 14.55w \log e_o \quad (18)$$

The coefficients of multiple determination for (a) and (b) are 0.63 and 0.97, respectively. From this relationship, for a given compaction energy level and initial void ratio, the effective stress-strength intercept (c') increases with moisture content. Also higher c' values were obtained for samples in which compression (rather than swelling) was achieved after saturation and consolidation.

PREDICTION PROCEDURES

In this study, the shear strength behavior of the laboratory- and field-compacted soils are similar but not identical. Thus there is a need to develop a procedure for predicting the shear strength behavior of field-compacted soils from laboratory-compacted data. Once correlations between field and laboratory shear strength characteristics for a particular soil exist, field responses can be predicted by running the desired laboratory test and substituting the relevant correlations.

However, if a situation obtains in which the laboratory soil is different from the field soil, although of the same geological origin, then there is a need to predict the laboratory control curve for the field soil. This can be accomplished by performing a laboratory-compaction test on the field soil at an energy level identical to that used for the laboratory soil. Assuming that the specific gravity of both soils are identical, at a given degree of saturation, and in accordance with Equations 10 and 11, the ratio of the laboratory soil moisture content to field soil moisture content is equal to the ratio of their corresponding void ratios. Thus, with this ratio known, translated water content and void ratios can be obtained for the field soil. The regression relationships for the shear strength parameters of the laboratory soil can be adjusted to give the laboratory control relationships for the field soil. Using relationships similar to those given in Equations 19 to 22, field shear responses could be estimated.

STATISTICAL REGRESSION

This procedure allows the generation of shear strength parameters of a field-compacted soil from the results, similar to those obtained in this study on laboratory-compacted soil. The field soil in question must be of the same geological origin as the laboratory one.

Reasonable populations of the desired laboratory shear strength parameters were established from the relevant relationship using the necessary independent variables. Using the field relationships, the translated moisture content, void ratio, and other independent variables, the equivalent field-compacted soil shear strength parameters were also determined for this study. A correlation between the field and laboratory parameters has been generated using statistical regression analysis.

(a) Dry density wet of optimum moisture content

$$\rho_d \text{ (field compacted)} = 188.3 + 0.872\rho_d \text{ (lab)} \quad (19)$$
$$R^2 = 0.88$$

where ρ_d is in kg/m^3, q_c in kPa, and $\Delta V/V_o$ in percent. Similar correlations could also be effected for dry of optimum moisture content.

(b) Unconsolidated undrained strength (q_c)

$$q_c \text{ (field)} = 174.92 + 0.916q_c \text{ (lab)} \quad (20)$$
$$R^2 = 0.84$$

(c) Volumetric strain due to saturation and consolidation

$$\Delta V/V_o\% \text{ (field)} = 1.886 + 0.495\Delta V/V_o\% \text{ (lab)} \quad (21)$$
$$R^2 = 0.81$$

(d) Skempton's A parameter at failure (A_f)

$$A_f \text{ (field)} = 0.223 + 0.66A_f \text{ (lab)} \quad (22)$$
$$R^2 = 0.69$$

(e) Effective stress-strength parameters: No correlations were established for the effective stress-strength intercept (c') and friction angle (ϕ'). Field responses can be estimated by judiciously adjusting the laboratory values based on field conditions.

CONCLUSIONS

1. A similarity exists in the shear strength behavior of field- and laboratory-compacted soils. These are manifested in the regression relationships generated for the various shear strength parameters.

2. The shear strength parameters P_s, q_c, $\Delta V/V_o$, A_f, ϕ', and c' can be expressed as functions of the relevant initial compaction variables. See Equations 5, 6, 8, 9, and 12-18.

3. A method for the prediction of field response from laboratory tests (where the soils are similar but not identical) has been developed.

REFERENCES

1. D.W. Weitzel and C.W. Lovell. The Effect of Laboratory Compaction on the Unconsolidated-Undrained Strength Behavior of a Highly Plastic Clay. Report 79-11. Joint Highway Research Project, 1979, Purdue University, West Lafayette, Ind., 218 pp.
2. J.M. Johnson and C.W. Lovell. The Effect of Laboratory Compaction on the Shear Behavior of a Highly Plastic Clay After Saturation and Consolidation. Report 79-7. Joint Highway Research Project, 1979, Purdue University, West Lafayette, Ind., 269 pp.
3. Y.C. Liang and C.W. Lovell. Strength of Field Compacted Clayey Embankments. Report 82-1. Joint Highway Research Project, 1982, Purdue University, West Lafayette, Ind., 312 pp.
4. P.S. Lin and C.W. Lovell. Compressibility of Field Compacted Clay. Report 81-14. Joint Highway Research Project, 1981, Purdue University, West Lafayette, Ind., 154 pp.
5. A. DiBernardo and C.W. Lovell. The Effect of Laboratory Compaction on the Compressibility of a Compacted Highly Plastic Clay. Report 79-3. Joint Highway Research Project, 1979, Purdue University, West Lafayette, Ind., 187 pp.
6. C.W. Lovell. Compacted Embankments: Predicting Field Compacted Behavior from Laboratory Compacted Samples. 19th Idaho Conference on Engineering Geology and Soil Engineering, Pocatello, April 1982, pp. 85-97.
7. R.J. Hodek and C.W. Lovell. A New Look at Compaction Processes in Fills. Bull., Association of Engineering Geologists, Vol. CVI, No. 4, 1979, Dallas, Tex., pp. 487-499.
8. P.T. Dacruz. Shear Strength Characteristics of Some Residual Compacted Clays. 2nd Pan-American Conference on Soil Mechanics and Foundation Engineering, Vol. 1, 1963, Rio de Janeiro, pp. 73-102.
9. D.J. Henkel. The Effect of Overconsolidation on the Behavior of Clays During Shear. Geotechnique, Vol. 6, No. 4, 1956, pp. 139-150.

Publication of this paper sponsored by Committee on Earthwork Construction.